

The Defect Detection and Non-Destructive Evaluation in Weld Zone of Austenitic Stainless Steel 304 Using Neural Network-Ultrasonic Wave

Won Yi* and In-Sik Yun**

(Received May 18, 1998)

In recent years, the importance of non-destructive evaluation has rapidly increased due to the collapse of large structures and the shooting up of safety accidents. The ultrasonic method, which is often used as a major non-destructive testing (NDT) technique in many engineering fields, is playing a significant role as a volumetric test regarded highly for evaluating a material's integrity. This paper is recommended for publication the detecting any defects of the weld zone in austenitic stainless steel type 304 using ultrasonic waves, employing neural network on the basis of the detected defects and evaluating them. In detecting defects, we drew a distance amplitude curve on a standard scan sensitivity and a preliminary scan sensitivity shown in the correlation between the ultrasonic probe, the instrument and the materials on a quantitative standard, and quantitative evaluation is used to draw a distance amplitude curve. A total of 93.3% of the defect types was distinguished by testing 30 defects after organizing a neural network system based on the defects on the ultrasonic evaluation and learning the neural network system. Thus the proposed ultrasonic wave-neural network in this work is useful for defects detection and Ultrasonic Non-Destructive Evaluation (UNDE) of the weld zone of austenitic stainless steel 304.

Key Words: Neural Network, Ultrasonic Wave, Ultrasonic Non-Destructive Evaluation, Shear Wave, Longitudinal Wave, Heat Affected Zone, Artificial Defect, Reference Block, Beam Distance, Refraction Angle

1. Introduction

There is a high occurability of surface and internal defects in the weld zone due to numerous variables in welding process. Among the defects, undercuts and cracks are subject to considerable stress concentration, thus often cause strength reduction.

Therefore, detecting various defects in the weld zone and quantitative evaluating are of great importance in terms of the structure's integrity and stability. The ultrasonic evaluation method, which is widely used to detect internal defects of

weld zone in many industry fields, plays an essential role as a volume testing method (ASME, 1995) among non-destructive testing methods performed in pre-/in-service (PSI/ISI) periods of chemical, thermal and atomic power plants.

Ultrasonic Non-Destructive Evaluation (UNDE) in weld zone for assuring the stability has great engineering significance for checking on and extending the life time of newly built pipe lines (along with the increased use of austenitic stainless steel) and pipe lines of presently operating atomic power plants. Studies on this include the radiographic testing method (Thomas et al., 1992), penetrant testing method (ASME, 1995), magnetic particle testing method (ASME, 1995) and ultrasonic testing method (Yi et al., 1996). Among these methods, the radiographic testing method has difficulties in real time result process-

* Department of Mechanical Engineering, Soongsil University

** Graduate School, Soongsil University/Korea Inspection & Engineering Co.

ing and in atomic damage. Penetrant testing and magnetic particle testing methods have a number of problems such as the limitations of defect detection to the surface and subsurface. However, the ultrasonic testing method (Yi et al., 1995, 1997, 1997) has advantages of detecting the location, size and even the pattern of the defects by employing the neural network whose superiority has been proven in the pattern recognition field. Studies on this have been done by Schmerr (1995) and Lee (1995), etc.

Schmerr (1995) categorized welding defects with ultrasonic pattern recognition method using Probabilistic Neural Network. Yi (1995) proposed an ultrasonic method with high site characteristics and practicability, and classified and evaluated artificial defects in heat affected zones with a neural network of back-propagation and learning algorithm.

The previous studies are mostly fragmentary and experimental on deposited metal and heat affected zones of the austenitic stainless steel 304 weld zone. There are a few studies on the detection and classification of defects in weld zone based on the quantitative defect evaluation standard with high practicability.

The weld zone of austenitic stainless steel is a coarse grain columnar structure. When ultrasonic waves propagate through the material, attenuation by scattering is high and signal-to-noise ratio is low due to many false echoes. Also, the columnar structures are considerably anisotropic affecting the shear wave to act as a guide wave leading to problems such as false echoes.

Thus, it is known that applying a shear wave angle method, which is an ultrasonic testing method employed in ferrite such as the existing carbon steel, only enables the detection of defects in the vicinity boundaries between the base metal and the deposited metal (Kishiyue, 1985), and that defect detection in deposited metal and its quantitative evaluation is almost impossible.

This study presents the defect classification and the Ultrasonic Non-Destructive Evaluation method on artificial defects (horizontal hole, vertical hole and notch) in the weld zone of austenitic stainless steel 304 by understanding the character-

istics of ultrasonic defect signals on CRT and constructing neural circuit network system, whose performance as a defect classifier is recently proven, from the acquired defect signals.

2. Theory of Neural Networks

2.1 Architecture of neural network & learning algorithm

A neural network simplifies biological neural cells in the human brain and their connective relations and then mathematically models them realizing an intelligent form the same as the human brain's parallel system.

Multilayer neural networks that is consisted of an input layer, a hidden layer and an output layer is used for pattern classification.

The mid layer and output layer have processing units and connection strength. The processing unit of each node processes an output through a sigmoid function $f(x)$ shown in Eq. (1) by adding bias value to each input value multiplied by strength.

$$f(x) = \frac{1}{1 + e^{(-x/\theta_0)}} \quad (1)$$

Where θ_0 is the shape factor determining the form of the sigmoid curve which is an activation function. The total input in each node, except in the input layer, is the values multiplied by the strength to the output values of all the nodes in the previous layers. That is, the total input in j th node in k th layer is as shown in Eq. (2).

$$net_j^k = \sum_{i=1}^m w_{ji}^k o_i^{k-1} \quad (2)$$

Where m is the node number in $(k-1)$ th layer, w_{ji}^k is the connection strength between i th node in $(k-1)$ th layer and j th node in k th layer, o_i^{k-1} is the output of i th node in $(k-1)$ th layer. Thus, the output from j th node of k th layer is as shown in Eq. (3).

$$o_j^k = \frac{1}{1 + e^{-(net_j^k + \theta_j)/\theta_c}} \quad (3)$$

In Eq. (3), the coefficient θ_j is the bias value. The node output in the hidden layer is calculated as in Eq. (3) and the output from the output node is calculated. The process is repeated to correct

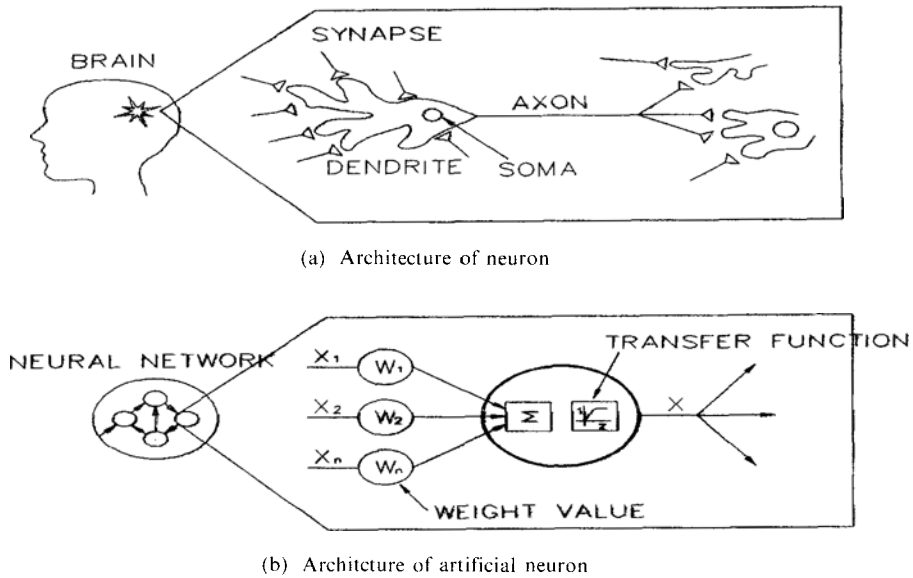


Fig. 1 Architecture of multilayer neural networks.

the connection strength between input and output nodes towards minimizing error E whose average is the square error equation term of the presumed value made according to each input pattern of the given output node. In general, the output value is different from the target value, so average system error can be calculated as below.

$$E = \frac{1}{2m} \sum_{i=1}^m (y_i - o_i)^2 \tag{4}$$

Where m is the number of data patterns assigned by input, y_i is the target value and o_i is the output value.

Minimizing the value of Eq. (4) against the connection strength w_j is made possible by the steepest-descent method, and the back-propagation algorithm is used.

$$w_{ji}^k(n+1) = w_{ji}^k(n) + \Delta w_{ji}^k(n) \tag{5}$$

$$\Delta w_{ji}^k(n) = -\eta \frac{\partial E}{\partial w_{ji}^k} \tag{6}$$

In Eqs. (5) and (6), a new strength is formed simply to execute the steepest descent on the current strength and the extent is adjusted by the learning rate η . If η is large, fast learning is adopted. But, E can be divergence in case of a complicated function against w_{ji}^k , thus a corrected learning formula with a momentum term is adopted as shown in Eq. (7).

$$\Delta w_{ji}^k(n+1) = -\eta \frac{\partial E}{\partial w_{ji}^k} + \alpha \Delta w_{ji}^k(n) \tag{7}$$

Where α is the momentum rate. It is the rate of using w_{ji} , estimated in the previous phase, and in the current phase in order to prevent the learning strength w_{ji} of the $(n+1)$ phase from differing dramatically from its value in the Italic phase.

2.2 Characterization of multilayer neural network

The characterizations of multilayer neural networks are, in large part, categorized as below.

- (1) Learning discrete finite input/output relations of finite numbers and networks simulating random successive maps can be constructed.
- (2) Even unlearned input data can be interpolated in the network and appropriate output can be acquired.
- (3) After learning is finished, a speedy output on given input data can be made through addition and multiplication by a processing unit.

Among the above categories, the 3rd characteristics enables the neural network to exercise its strongest points most effectively by evaluating an object, requiring high-speed process, with precision.

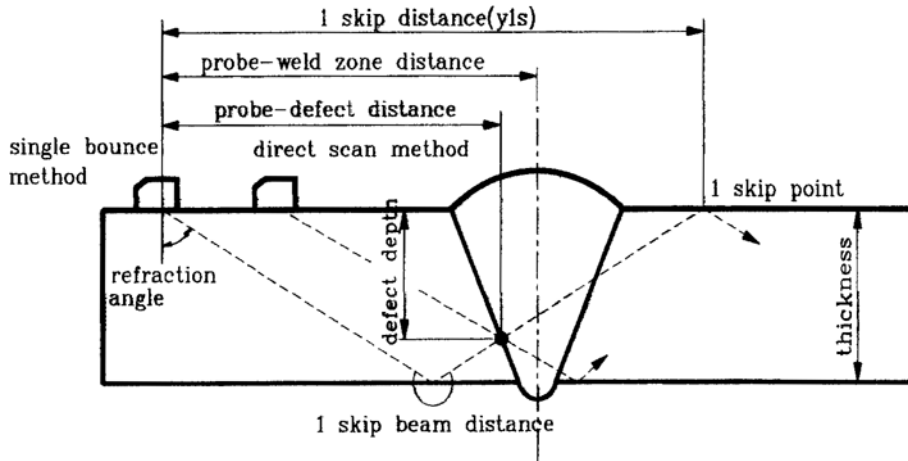


Fig. 2 Principle of angle beam method.

3. Theory of Ultrasonic wave

Among the sound waves propagating through solid objects, there are longitudinal waves, whose particles' vibration is in the same direction as the waves, and the shear waves, whose particles move perpendicularly to the waves. The sound velocity is determined by the type and characteristics of the material the waves go through.

The C_l , the sound velocity of longitudinal waves, and C_s , the sound velocity of shear waves, are shown in Eqs. (8) and (9), respectively.

$$C_l = \sqrt{\frac{E}{\rho} \times \frac{(1-\nu)}{(1+\nu)(1-2\nu)}} = \sqrt{\frac{K + (4/3)G}{\rho}} \quad (8)$$

$$C_s = \sqrt{\frac{E}{\rho} \times \frac{1}{2(1+\nu)}} = \sqrt{\frac{G}{\rho}} \quad (9)$$

where E is Young's modulus, K is bulk modulus, G is shear modulus, ρ is density and ν is Poisson's ratio.

Ultrasonic waves for defect detecting purposes propagate through a material with a constant velocity and acquire reflective echoes from defects. In case weld zone defects are subject to the test, angle beam ultrasonic inspection utilizing the refraction angle of a probe can be applied. Regarding the direct method based on 0.5 skip beam distance limit, the following formulas can be drawn up according to the principle of trigonometric function and the principle is shown

in Fig. 2.

$$W_{0.5s} = \frac{t}{\cos \theta} \quad (10)$$

$$y = W \sin \theta \quad (11)$$

$$d = W \cos \theta \quad (12)$$

$$d' = 2t - W \cos \theta \quad (13)$$

Where the skip point is where the beam central axis reflected from the back surface reaches the scanning surface in an angle scan. Beam distance (W) is the distance the ultrasonic wave beam moved, 1 skip beam distance is the distance from incident point of the probe to the 1 skip point, and 0.5 skip distance is the distance to the 0.5 skip point. In Eq. (13), the defect depth detected by the 1 time reflection method indicates $d' = 2t - W \cos \theta$, and this is the distance measured by presuming the plate to be twice as thick.

4. Experiments

4.1 Experimental Conditions

The main instruments used for this study are an ultrasonic instrument (Epoch II of Panametrics Co.), a shear wave angle probe (Krautkramer Co. frequency : 2MHz, refraction angle : 70°, piezoelectric size: 8×9mm), a longitudinal wave angle probe (New Japan Non-Destructive Testing Co. frequency : 2MHz, refraction angle : 70°, piezoelectric size: 20×35mm), a normal probe (Krautkramer Co. frequency : 2MHz, piezoelectric

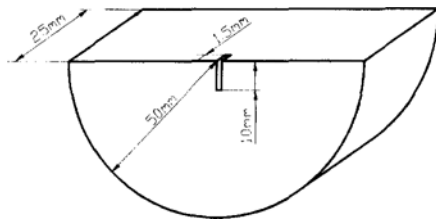


Fig. 3 Configuration of reference block (ITRB).

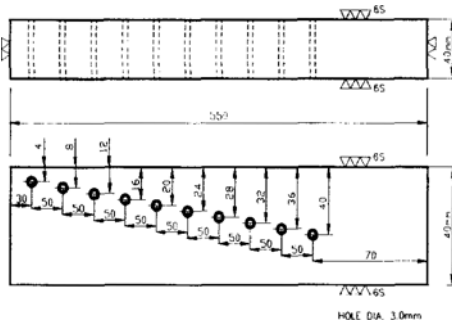


Fig. 4 Configuration of reference block (RDRB).

size: ϕ 10mm), and mechanical oil (Yun et al., 1996). In the experiments, we tried to understand the echo characteristics on the CRT of the ultrasonic instrument by the correlations among the refraction angles of vertical and angle probes, frequency, the thickness of the test piece and its property. For these, we built a reference block as shown in Figs. 3 and 4. Fig. 3 shows the reference block for adjustment of the incident point and the time axis, and Fig. 4 shows the reference block to measure the refraction angle and calibrating the ultrasonic instrument.

For quantitative defect detection of austenitic stainless steel 304 weld zone using ultrasonic waves, selecting test piece with the same properties and thickness as the materials to be tested and processing it with the same welding condition are necessary. To this end, three types of artificial defects such as horizontal hole, vertical hole and notch are processed in the heat affected zone and the deposited metal of the test piece as shown in Figs. 5 and 6.

4.2 Setting of distance amplitude curve (DAC)

To use ultrasonic waves for defect detection

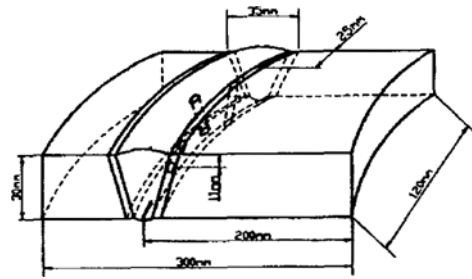


Fig. 5 Configuration of standard test block.

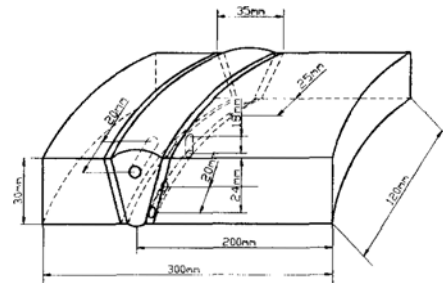


Fig. 6 Configuration of test block.

purposes inside a material, setting quantitative defect detection standards is required, and DAC is applied as the standard. Thus, the level DAC is set to affect the detectability of defects, and it is mapped out with the echodynamic patterns displayed on the CRT of the ultrasonic instrument as factors.

For this, it is directly drawn up on the CRT of the ultrasonic instrument on the basis of the reflected echo from the horizontal hole of the RDRB in the pulse-echo method.

The major points of consideration and the method of drawing it up are as follows :

- Selecting the frequency and refraction angle of the probe in consideration of the condition of the materials to be tested.
- Measuring the real refraction angle and the incident point of the probe
- Measuring the maximum echo location on the horizontal hole of each RDRB
- Setting the height of standard echo against the maximum echo

5. Experiment and Simulation Results

5.1 Ultrasonic characterization in weld zone

The weld zone of austenitic stainless steel has a coarse grain columnar structure. When ultrasonic waves propagate through the weld zone, attenuation of ultrasonic wave by scattering is high, signal-to-noise ratio is low since the columnar structures are considerably anisotropic, and false echoes appear. All these characteristics present noticeable differences from ferrite carbon steel.

For quantitative defect detection, precise calibration of the ultrasonic instrument and the probe is indispensable. To satisfy this, the ultrasonic instrument and the probe using ITRB and RDRB were calibrated and attempted to determine the detection likelihood on horizontal hole defects in the middle of the weld zone as in Fig. 6 using the shear wave angle method. The results are shown in Fig. 7.

The far left signal with echo height of more than 100% is transmitted an echo and the three solid lines indicate DAC with 6dB intervals. When drawing up the DAC, the standard sensitivity is set at 50.7dB, and the preliminary scan sensitivity is set at 68.7dB, 18dB higher than the standard sensitivity. The location of the defect echo shown as 55% in the determined gate zone on the CRT in the deposited metal indicates propagated beam distance, the surface distance from the probe to the defect and the depth. But the truly measured beam distance and depth are 38.82mm and 14.54mm, respectively, different values from the indicated value on the CRT. Considering that there are no defects around the horizontal

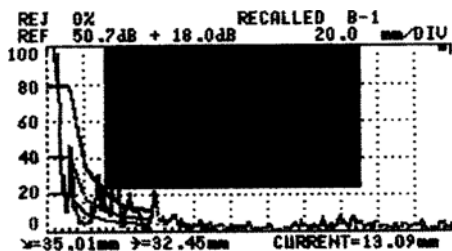


Fig. 7 Results of defect echo in deposited metal.

hole to show through the defect echo, it is presumed that when ultrasonic waves propagate through the columnar-structured deposited metal, they act as guided wave and are guided rather than going-toward defects and returned after striking the surface as false echoes.

When detecting defects in deposited metal, it is important to understand the changes in ultrasonic wave echoes in the direct method using a longitudinal wave angle probe, which is different from those in the shear wave angle method. Fig. 8 shows the echo behavior of the ultrasonic waves against the side hole and the vertical hole. It is noticeable that the ultrasonic echo on the CRT against the side hole and vertical hole is very similar to the measured distance, and the standard sensitivity (40.4dB), the preliminary scan sensitivity (58.4dB), time axis (100mm) and DAC are assigned markedly differently from in the case of the shear wave angle method.

The echo behavior differs depending on the size and type of the defect and the traveled beam distance, and this influences the detectability of defects most greatly.

Figs. 10 and 11 show a phenomenon. In Fig.

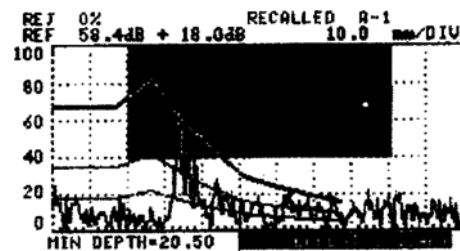


Fig. 8 Results of 3.0mm vertical hole in deposited metal.

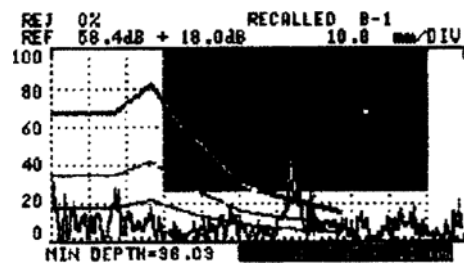


Fig. 9 Results of 3.0mm vertical hole in deposited metal.

10, especially, the reflected echo returning from the near surface of the vertical hole with a 1 skip beam distance is displayed to be remarkably small.

Fig. 11 presents the result of the surface notch which is about 1 skip beam distance. The propagated beam distance is similar to that of

Fig. 10, but the height of the echo is 24%, twice as high. This is to indicate that even though ultrasonic waves propagate the same distance, differences are made owing to the strong correlations among the defect type, the reflection form and the sizes.

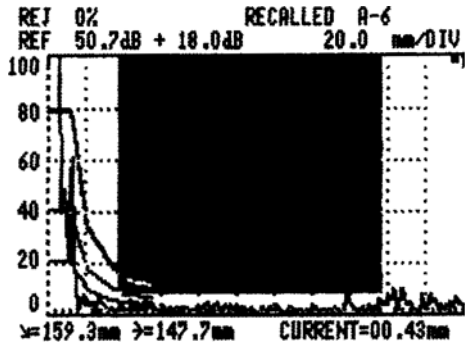


Fig. 10 Results of 3.0mm vertical hole.

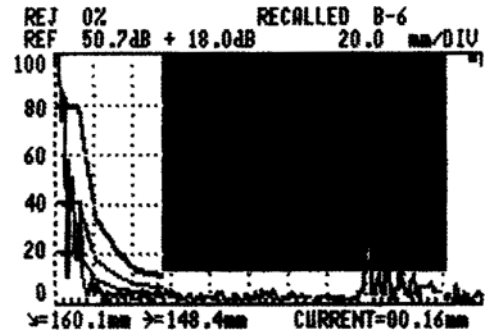


Fig. 11 Results of notch.

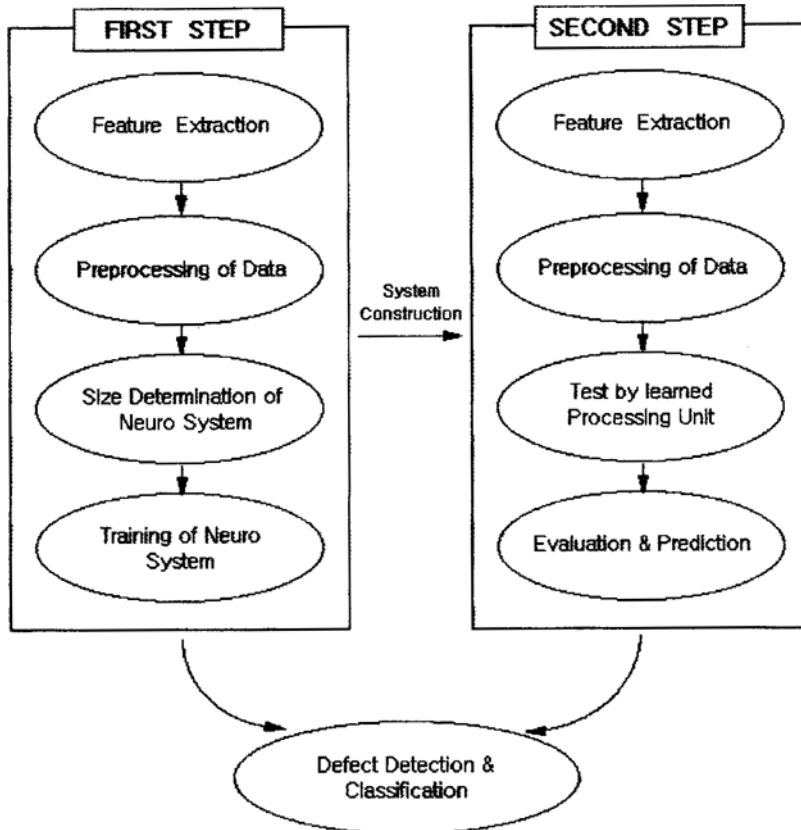


Fig. 12 Constitution of total system for defect analysis.

5.2 Configuration of neural network system for the classification of welding defects

This study applied multilayer neural network with back-propagation learning algorithm whose validity is proven in recent non-linear analysis.

The configuration of the whole system consists of two stages as shown in Fig. 12, where major subjects for interpretation are mostly determined in stage 1.

The subjects dealt with in stage 1 are: 1) concern defects in the austenitic stainless steel 304 weld zone and to, acquire the echodynamic pattern information of ultrasonic waves on each measuring points in the skip distance of 0.5 ~ 1.0; 2) to select and extract the optimum features of the acquired information; 3) to regard the determined features, pre-process the data by normalizing it based on the maximum real value; 4) determine subjects relating to the input layer, hidden layer and output layer; 5) the system is completed as the weight coefficient values of each layer are determined through a learning process.

In stage 2, by utilizing the established system in stage 1; 1) the features are selected and extracted from the information of defects with different ultrasonic wave beam distances and locations; 2) regarding the determined features, pre-process the data normalized against the maximum real value considering the standard applied during a learning process; 3) to test it through addition and multiplication with a learned processing unit; 4) finally to carry out ultrasonic non-destructive evaluation and prediction on defects by calculating the error rate on the basis of the success recognition rate on the patterns (90% of target value).

The above process can be made speedily using a parallel computer or an exclusive neuro computer. Since the size of the system differs depending on the subject to analyze, when a simple analysis to be done, a small computer is recommended to achieve real time process results due to the small calculation size.

5.3 Classification and evaluation of defects in neural network

The neural network is a system which learns

several sample data and conjectures output information from input information on unlearned data. In this study, a defect classification system was constructed with ultrasonic signals as the data.

The structure and input condition of the applied neural network are each shown in Tables 1 and 2. The learning rate and momentum term are determined through numerous repetitive simulation based on the convergency of execution time and solution in order to carry out the optimal condition of the neural network system and Fig. 13 shows the process of solution convergence. As executing the program, it is increased toward 0.27 in the beginning, is gradually converged after

Table 1 Structure of neural network for training.

| Parameters | Structure |
|-----------------------------|-----------|
| Number of input units | 4 |
| Number of hidden units | 12 |
| Number of output units | 3 |
| Number of hidden layers | 1 |
| Learning rate (η) | 0.7 |
| Momentum rate (γ) | 0.9 |
| Shape factor ($\theta 0$) | 1.0 |

Table 2 Relation of defect and defect type.

| Defect | Defect type |
|---------------------------------|-------------|
| $\phi 3\text{mm}$ side hole | 1 |
| $\phi 3\text{mm}$ vertical hole | 2 |
| Notch | 3 |

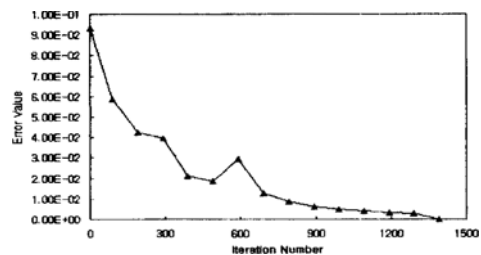


Fig. 13 Process of error convergence in constitution neuro system.

passing the point, shows a momentary error increase at 12,000 repetition number point, stabilize at about 27,000 point, and finally converges close to the target value.

The way to recognize a defect type is to have a target value on each defect using binary code on 2 patterns.

The structure and input condition of the

Table 3 Learning condition and results.

| Experimental conditions | | | | Actual defect types | | | Defect type of learning results | | |
|-------------------------|-----------|-----------------------|-------------|---------------------|---|---|---------------------------------|------|------|
| Beam distance | Frequency | Real refraction angle | Echo height | 1 | 2 | 3 | 1 | 2 | 3 |
| 0.107 | 1.00 | 1.00 | 100 | 1 | 0 | 0 | 0.99 | 0 | 0 |
| 0.119 | 1.00 | 1.00 | 100 | 1 | 0 | 0 | 0.99 | 0 | 0 |
| 0.137 | 1.00 | 1.00 | 100 | 1 | 0 | 0 | 0.99 | 0 | 0 |
| 0.197 | 0.90 | 0.99 | 75 | 1 | 0 | 0 | 0.99 | 0 | 0 |
| 0.225 | 0.90 | 0.99 | 72 | 1 | 0 | 0 | 0.99 | 0 | 0 |
| 0.269 | 0.90 | 0.99 | 56 | 1 | 0 | 0 | 0.99 | 0 | 0 |
| 0.309 | 0.90 | 0.99 | 41 | 1 | 0 | 0 | 0.99 | 0 | 0 |
| 0.340 | 0.90 | 0.99 | 40 | 1 | 0 | 0 | 0.99 | 0 | 0 |
| 0.781 | 1.00 | 1.00 | 35 | 1 | 0 | 0 | 0.99 | 0 | 0 |
| 0.829 | 1.00 | 1.00 | 25 | 1 | 0 | 0 | 0.99 | 0 | 0 |
| 0.221 | 1.00 | 1.00 | 35 | 0 | 1 | 0 | 0 | 0.99 | 0 |
| 0.263 | 1.00 | 1.00 | 30 | 0 | 1 | 0 | 0 | 0.99 | 0 |
| 0.376 | 0.90 | 0.99 | 43 | 0 | 1 | 0 | 0 | 0.99 | 0 |
| 0.423 | 0.90 | 0.99 | 70 | 0 | 1 | 0 | 0 | 0.99 | 0 |
| 0.489 | 0.90 | 0.99 | 57 | 0 | 1 | 0 | 0 | 0.99 | 0 |
| 0.538 | 0.90 | 0.99 | 35 | 0 | 1 | 0 | 0 | 0.99 | 0 |
| 0.585 | 1.00 | 1.00 | 35 | 0 | 1 | 0 | 0 | 0.99 | 0 |
| 0.621 | 1.00 | 1.00 | 30 | 0 | 1 | 0 | 0 | 0.99 | 0 |
| 0.769 | 1.00 | 1.00 | 17 | 0 | 1 | 0 | 0 | 0.99 | 0 |
| 0.950 | 1.00 | 1.00 | 10 | 0 | 1 | 0 | 0 | 0.99 | 0 |
| 0.393 | 0.90 | 0.99 | 43 | 0 | 0 | 1 | 0 | 0 | 0.98 |
| 0.400 | 0.90 | 0.99 | 45 | 0 | 0 | 1 | 0 | 0 | 0.99 |
| 0.413 | 0.90 | 0.99 | 60 | 0 | 0 | 1 | 0 | 0 | 0.99 |
| 0.436 | 1.00 | 1.00 | 20 | 0 | 0 | 1 | 0 | 0 | 0.99 |
| 0.483 | 1.00 | 1.00 | 15 | 0 | 0 | 1 | 0 | 0 | 0.99 |
| 0.507 | 1.00 | 1.00 | 15 | 0 | 0 | 1 | 0 | 0 | 0.99 |
| 0.542 | 0.90 | 0.99 | 75 | 0 | 0 | 1 | 0 | 0 | 0.99 |
| 0.890 | 1.00 | 1.00 | 30 | 0 | 0 | 1 | 0 | 0 | 0.99 |
| 0.937 | 1.00 | 1.00 | 28 | 0 | 0 | 1 | 0 | 0 | 0.99 |
| 0.990 | 1.00 | 1.00 | 17 | 0 | 0 | 1 | 0 | 0 | 0.99 |

applied neural network are shown in Tables 1 and 2.

The size of the layer type neural network is related directly to the operation amount analyzing the features of the constructed system. Finally it was set as 99% in consideration of the combined total number between the input layer, the hidden layer and the output layer. The optimization of the system on this took 147 seconds.

The neural network learns using a back-propagation learning algorithm with the following as samples: the beam distance from the probe to a defect, the frequency features of shear and longitudinal angle probes, measured refraction angle relation and the defect type depending on echo height.

Learning was carried out by setting the total error value as 0.0001 with 30 patterns as sample data and with 30,000 learning numbers, and the learning result turned out with about 99% accuracy so that is almost identical to the target value except the pattern on 1 notch (98%). The learning result of defect recognition according to the input pattern is shown in Table 3.

Also, after testing a new experimental condition(welding defect with different location and distance) with learned processing units, the value was evaluated below 90% of target value on an

error processing standard basis.

Table 4 is the test result on a side hole, and a 90% of success rate was indicated as the 2nd data out of 10 was 0.41 and was processed as an error. In the result on the vertical hole in Table 5, only the data on the bottom line was 0.89 and showed a 90% of success rate as in the case of the side hole. In the case of side hole, the pattern judged to be an error was 0.58 and it indicates a result of

Table 5 Test result of vertical hole.

| Experimental conditions | | | | Defect type of learning results | | | Actual defect types |
|-------------------------|-----------|-----------------------|-------------|---------------------------------|------|------|---------------------|
| Beam distance | Frequency | Real refraction angle | Echo height | 1 | 2 | 3 | |
| 0.466 | 0.90 | 0.99 | 40 | 0 | 0.92 | 0.07 | 2 |
| 0.495 | 1.00 | 1.00 | 35 | 0 | 0.99 | 0 | 2 |
| 0.530 | 1.00 | 1.00 | 35 | 0 | 0.99 | 0 | 2 |
| 0.566 | 1.00 | 1.00 | 35 | 0 | 0.99 | 0 | 2 |
| 0.614 | 0.90 | 0.99 | 30 | 0 | 0.99 | 0 | 2 |
| 0.662 | 0.90 | 0.99 | 25 | 0 | 0.99 | 0 | 2 |
| 0.441 | 0.90 | 0.99 | 75 | 0 | 0.99 | 0 | 2 |
| 0.456 | 0.90 | 0.99 | 70 | 0 | 0.99 | 0 | 2 |
| 0.565 | 0.90 | 0.99 | 65 | 0 | 0.99 | 0 | 2 |
| 0.513 | 0.90 | 0.99 | 50 | 0 | 0.89 | 0.11 | 2 |

Table 4 Test result of side hole.

| Experimental conditions | | | | Defect type of learning results | | | Actual defect types |
|-------------------------|-----------|-----------------------|-------------|---------------------------------|------|---|---------------------|
| Beam distance | Frequency | Real refraction angle | Echo height | 1 | 2 | 3 | |
| 0.352 | 1.00 | 1.00 | 70 | 0.99 | 0 | 0 | 1 |
| 0.436 | 1.00 | 1.00 | 70 | 0.41 | 0.58 | 0 | 1 |
| 0.209 | 0.90 | 0.99 | 75 | 0.99 | 0 | 0 | 1 |
| 0.229 | 0.90 | 0.99 | 69 | 0.99 | 0 | 0 | 1 |
| 0.239 | 0.90 | 0.99 | 65 | 0.99 | 0 | 0 | 1 |
| 0.251 | 0.90 | 0.99 | 62 | 0.99 | 0 | 0 | 1 |
| 0.261 | 0.90 | 0.99 | 60 | 0.99 | 0 | 0 | 1 |
| 0.282 | 0.90 | 0.99 | 53 | 0.99 | 0 | 0 | 1 |
| 0.291 | 0.90 | 0.99 | 48 | 0.99 | 0 | 0 | 1 |
| 0.298 | 0.90 | 0.99 | 45 | 0.99 | 0 | 0 | 1 |

Table 6 Test result of notch Experimental conditions.

| Experimental conditions | | | | Defect type of learning results | | | Actual defect types |
|-------------------------|-----------|-----------------------|-------------|---------------------------------|---|------|---------------------|
| Beam distance | Frequency | Real refraction angle | Echo height | 1 | 2 | 3 | |
| 0.913 | 1.00 | 1.00 | 28 | 0 | 0 | 0.98 | 3 |
| 0.925 | 1.00 | 1.00 | 28 | 0 | 0 | 0.99 | 3 |
| 0.955 | 1.00 | 1.00 | 25 | 0 | 0 | 0.99 | 3 |
| 0.968 | 1.00 | 1.00 | 22 | 0 | 0 | 0.99 | 3 |
| 0.986 | 1.00 | 1.00 | 20 | 0 | 0 | 0.99 | 3 |
| 0.485 | 0.90 | 0.99 | 99 | 0 | 0 | 0.99 | 3 |
| 0.498 | 0.90 | 0.99 | 95 | 0 | 0 | 0.99 | 3 |
| 0.508 | 0.90 | 0.99 | 92 | 0 | 0 | 0.99 | 3 |
| 0.520 | 0.90 | 0.99 | 88 | 0 | 0 | 0.99 | 3 |
| 0.531 | 0.90 | 0.99 | 83 | 0 | 0 | 0.99 | 3 |

only 40% of recognition. This is thought to be a case extremely out of the learning range considering the features of the neural network indicating interpolation and extrapolation.

In the test result on the notch as shown in Table 6, all 10 data were 0.99 close to target value, and thus 100% of success rate was recorded.

It is able to be verified that the neural network constructed in this study is useful for defect classification of the austenitic stainless steel 304 weld zone, as the total success rate was as high as 93.3% even though 2 out of the total 30 data were judged to be errors.

6. Conclusion

It is a common view worldwide that the austenitic stainless steel 304 weld zone has a coarse grain columnar structure unlike the ferrite carbon steel. Thus, when detecting defects using ultrasonic waves, the detection and its evaluation are extremely difficult. In particular, the ultrasonic wave studies on defect detection in stainless steel in Korea are fragmentary and dragging with several detailed results.

Considering the situation, therefore, this study processed artificial defects (horizontal hole, vertical hole and notch) in austenitic stainless steel 304 welding test piece, inquired into the quantitative detection of welding defects with ultrasonic waves, had the multilayer neural network learn detected defects with back-propagation learning algorithm, tested and classified defect types, and achieved the following results.

(1) The possibility of defect detection in the deposited metal zone and the heat affected zone was verified by combining shear wave and longitudinal wave angle probes in ultrasonic testing for defect detection of the austenitic stainless steel 304 weld zone.

(2) Quantitative ultrasonic wave standard with practicability was introduced through detecting defects with standard scan sensitivity (50.7, 58.4dB) and preliminary scan sensitivity (68.7, 76.4dB) of DAC against deposited metal and heat affected zone.

(3) After a test was conducted with a processing unit the constructed neural network learned, success rate was 90% in side hole, 90% in vertical hole and 100% in notch, and the defect pattern was determined as a high success rate of 93.3% on the total of 30 patterns.

(4) A practical evaluation method was introduced for the future weld defect classification automation, as defect type was determined in the neural network composed of 99 systems.

Acknowledgement

This study is supported by academic research fund (ME97-C-19) of Ministry of Education, Republic of Korea. We would like to appreciate President Bang Y. H. of KIECO for their support and comments on this paper.

References

- ASME Boiler & Pressure Vessel Code Sec. XI, 1995, "Rules for Inservice Inspection of Nuclear Power Plant Components," pp. 287~319.
- Thomas F. Perrone, 1992, "Principles of Radiographic Film Interpretation of Pipeline Welds, Journal of the American Society for Nondestructive Testing," Vol. 50, 11, pp. 1268~1273.
- ASME Boiler & Pressure Vessel Code Sec. V, 1995, "Standard Practice for Liquid Penetrant Inspection Method," pp. 455~472.
- ASME Boiler & Pressure Vessel Code Sec. V, 1995, "Magnetic Particle Examination," pp. 151~156.
- Yi, W., Yun, I. S., Hwang, Y. T., Yu, Y. C. and Jeong, E. S., 1996, "Defect Detection and Evaluation of Weld Zone by Using Ultrasonic Method," *Proc. Fall Meeting, KSME in Korea*, Vol. I, pp. 41~46.
- Yi, W., Yun, I. S., Oh, S. Y., Yu, Y. C. and Jeong, E. S., 1995, "The Prediction and Evaluation of Ultrasonic Echo by Using Neural Network," *Proc. Fall Meeting, KSNT in Korea*, pp. 1~7.
- Yi, W., Yun, I. S., Yu, Y. C. and Jeong, E. S., 1997, "Defect Detection and Nondestructive Evaluation of Weld Zone in Austenitic Stainless Steel

Method," *Proc. Spring Meeting, KSME in Korea*, Vol. 1, pp. 236~241.

Yi, W., Yun, I. S., Yu, Y. C. and Jeong, E. S., 1997, "The Prediction and Evaluation of Ultrasonic Echo by Using Neural Network," *Trans of the KSME in Korea*, Vol. 21, No. 4, pp. 586~595.

Schmerr, L. W. and Song, S. J., 1995, "Ultrasonic Flaw Classification in Weldments Using Probabilistic Neural Networks," *Journal of Nondestructive Evaluation*, Vol. 11, pp. 395~406.

Lee, K. Y. and Kim, J. S., 1995, "Intelligence

Package Development for UT Signal Pattern Recognition and Application to Classification of Defects in Austenitic Stainless Steel Welds," *KSNT in Korea*, Vol. 15, No. 4, pp. 531~539.

Kishiue, 1985, "Guide Line for the Ultrasonic Testing Method of the Austenitic Stainless Steel Welds," *JSNDI*, Vol. 34, No. 2, pp. 60~76.

Yun, I. S., Lee, S. S., Kim, Y. H., Lee J. G. and Kim, H. C., 1996, "A Study on the Couplant Effects in Contact Ultrasonic Testing," *Proc. Spring Meeting, KSNT in Korea*, pp. 206~211.